

UNCLASSIFIED



**Australian Government**  
**Department of Defence**  
Defence Science and  
Technology Organisation

# Development of Photon Doppler Velocimeter for Explosives Research

*Valerian A. Kuznetsov and Shayne P. Bennetts*

**Weapons Systems Division**  
Defence Science and Technology Organisation

DSTO-TR-2792

## **ABSTRACT**

A Photon Doppler Velocimeter (PDV) was built for explosives research. The PDV is comprised of a 1550 nm continuous-wave single-mode fibre laser, an optical circulator, a photodetector and a GHz range capable oscilloscope. As a test, it was used to record the velocity history of the back surface of 5 mm thick steel plates driven by the detonation products of PE4 charges of mass 15 - 60 g. A bare fibre tip, located 1 - 4 mm away from the target was used as the optical probe. Time resolution of 7 ns was achieved. The free surface velocity effects were interpreted in terms of the elastic-plastic model of steel, Chapman-Jouguet pressure was evaluated, and Gurney equations were applied to describe the motion of the steel plate. The measurement limitations of the PDV system are determined, applications for explosives research are discussed, and the upgrade pathway is recommended.

## **RELEASE LIMITATION**

*Approved for public release*

UNCLASSIFIED

UNCLASSIFIED

*Published by*

*Weapons Systems Division  
DSTO Defence Science and Technology Organisation  
PO Box 1500  
Edinburgh South Australia 5111 Australia*

*Telephone: (08) 7389 5555  
Fax: (08) 7389 6567*

*© Commonwealth of Australia 2013  
AR-015-494  
January 2013*

**APPROVED FOR PUBLIC RELEASE**

UNCLASSIFIED

UNCLASSIFIED

# Development of Photon Doppler Velocimeter for Explosives Research (U)

## Executive Summary

Experimental methods of explosives research involve the determination of properties of the detonation wave as it propagates inside the explosive charge, as well as properties of the shockwaves propagating inside the inert materials adjacent to the detonated charge. Photon Doppler Velocimeter (PDV) can be used to measure the velocity of a shocked material's free surface with nanosecond resolution. Photon Doppler Velocimetry is a relatively novel technique which was first described by the Lawrence Livermore National Laboratory (LLNL) authors in *Review of Scientific Instruments* in 2006. The technique is based on mixing the light wave incident onto a moving target, with the reflected light of changed frequency. The frequency of the resulting beat wave is proportional to the velocity of the target. The technique is simple and relatively inexpensive compared to competing methods such as VISAR and Fabry-Perot interferometry.

This report describes the development of a PDV and an application of it to the measurement of the velocity of steel shocked by detonating a PE4 explosive charge. The PDV used a 100 mW 1550 nm infrared continuous wave single mode fibre laser, a circulator, a photodetector, and an oscilloscope of a 2.5 GHz bandwidth.

The obtained data allowed evaluation of the detonation pressure of PE4 and to measure the terminal velocity of a steel plate accelerated by the explosive. The maximum measurement velocity is 2-3 km/s, and the demonstrated time resolution is 7 ns.

The outcomes of the PDV trial show that the technique is working and can be applied to a range of explosives research problems. The PDV could be used in the cylinder expansion test where the acceleration of the cylinder wall under the pressure of the expanding detonation gases is measured, and the performance of the explosive is assessed. In another possible experiment, a flying plate test, the structure of the detonation wave could be studied by recording a velocity history of an interface between the explosive and a window.

UNCLASSIFIED

UNCLASSIFIED

*This page is intentionally blank*

UNCLASSIFIED

## Authors

### **Valerian A. Kuznetsov**

Weapons Systems Division



*Valerian obtained a BSc degree in Physics from Novosibirsk State University (Russia) in 1992, and a PhD degree in Physics from University of New South Wales (Australia) in 1998. His early career was on semiconductors and optics. Since joining DSTO in 2003, he conducted research in electromagnetism, explosive blast loading of structures, and currently in detonics.*

---

### **Shayne P. Bennetts**

Australian National University



*Shayne graduated with BSc in Physics from ANU in 2000. He worked in Electronic Warfare and Radar Division at DSTO on the development of fibre lasers. Shayne is currently undertaking his PhD studies in Physics at ANU.*

---

UNCLASSIFIED

*This page is intentionally blank*

UNCLASSIFIED

# Contents

## GLOSSARY

|  |           |
|--|-----------|
| <b>1. INTRODUCTION.....</b>  | <b>1</b>  |
| <b>1.1 Prior art velocimeters .....</b>                              | <b>1</b>  |
| <b>1.2 DSTO velocimeter .....</b>                                    | <b>1</b>  |
| <b>2. EXPERIMENTAL .....</b>   | <b>2</b>  |
| <b>2.1 Explosive charge assembly.....</b>                            | <b>2</b>  |
| <b>2.2 Photon Doppler Velocimeter.....</b>                           | <b>4</b>  |
| 2.2.1 Heterodyne theory .....  | 4         |
| 2.2.2 Implementation.....  | 5         |
| 2.2.3 Requirement for coherence .....                                | 7         |
| 2.2.4 Options for increasing the fibre-target range .....            | 8         |
| 2.2.5 Laser safety considerations .....                              | 8         |
| 2.2.6 Laser light-explosive interaction .....                        | 8         |
| 2.2.7 Data processing.....   | 8         |
| <b>3. RESULTS .....</b>  | <b>9</b>  |
| <b>3.1 Free surface velocity of metal plate .....</b>                | <b>9</b>  |
| <b>4. DISCUSSION .....</b>   | <b>13</b> |
| <b>4.1 Elastic and plastic waves in steel .....</b>                  | <b>13</b> |
| 4.1.1 Elastic-plastic model .....                                    | 13        |
| 4.1.2 Interpretation of free surface velocities .....                | 15        |
| <b>4.2 Velocity of steel plate.....</b>                              | <b>18</b> |
| 4.2.1 Gurney equation.....   | 18        |
| 4.2.2 Interpretation of plate velocity by Gurney formula .....       | 19        |
| <b>5. RECOMMENDATIONS.....</b>                                       | <b>20</b> |
| <b>5.1 Explosives research with Photon Doppler Velocimeter .....</b> | <b>20</b> |
| <b>6. CONCLUSIONS.....</b>   | <b>21</b> |
| <b>7. ACKNOWLEDGEMENTS .....</b>                                     | <b>21</b> |
| <b>8. REFERENCES .....</b>   | <b>22</b> |

UNCLASSIFIED

DSTO-TR-2792

*This page is intentionally blank*

UNCLASSIFIED



## Glossary

|       |  |
|-------|--|
| C-J   | Chapman-Jouguet (Pressure)                       |
| FFT   | Fast Fourier Transform                           |
| HEL   | Hugoniot Elastic Limit                           |
| LiF   | Lithium Fluoride                                 |
| LLNL  | Lawrence Livermore National Laboratory           |
| NOHD  | Nominal Ocular Hazard Distance                   |
| OD    | Optical Density                                  |
| PBX   | Polymer Bonded Explosive                         |
| PDV   | Photon Doppler Velocimeter                       |
| PE4   | Plastic Explosive No. 4                          |
| PETN  | Pentaerythritol Tetranitrate                     |
| PIR   | Phase Interface Reflection                       |
| PMMA  | Poly(Methyl Methacrylate)                        |
| TATB  | Triaminotrinitrobenzene                          |
| VISAR | Velocity Interferometer System for Any Reflector |

UNCLASSIFIED

DSTO-TR-2792

*This page is intentionally blank*

UNCLASSIFIED

# 1. Introduction

## 1.1 Prior art velocimeters

Diagnostics of detonation waves and of explosive blasts involves the determination of the velocity of a metal plate or of a metallised window interface. The velocities typically are several km/s. The velocimetry systems which have become most popular with the explosives research communities are Velocity Interferometer System for Any Reflector (VISAR) developed at Sandia National Laboratories in the late 1960s [1], and Fabry-Pérot interferometer developed at Lawrence Livermore National Laboratory (LLNL) in the 1980s [2].

Both systems are based on the determination of the velocity of fast-moving reflective surface by the Doppler shift of the reflected light, and they have their advantages and disadvantages due to their implementation. Both are rather expensive. For example, a VISAR commercially available from Valyn costs over US\$200k. Fabry-Perot is custom-built and costs even more. Both are susceptible to the variation of the intensity of the reflected light from the shocked surface. They could be susceptible to the abrupt change in velocity.

A development of a heterodyne velocimeter termed Photon Doppler Velocimeter (PDV) was reported by LLNL in 2006 [3]. This velocimetry system has some of the advantages of both VISAR and Fabry-Perot. The LLNL authors built it utilising commercial off-the-shelf components such as single-mode fibres and fibre devices, a 2W continuous wave 1550 nm infrared laser, and high-speed oscilloscope operating in GHz frequency range. The operation of the velocimeter is based on superimposing the incident and reflected Doppler-shifted light, and measuring the beat frequency, which is proportional to the velocity of the moving surface. The maximum velocity was 5 km/s, limited by the bandwidth of the chosen oscilloscope.

## 1.2 DSTO velocimeter

A similar PDV system has been developed at DSTO utilising the electronic components of a narrower bandwidth which had a routine availability from a radiofrequency laboratory. The maximum velocity was limited by about 2 km/s. A 100 mW continuous wave laser was used which was also routinely available from an optics laboratory due to its low ocular hazard, and due to a possibility to use the standard optical connectors. In the described work, the PDV performance was verified by the measurement of the velocity of PE4 explosively-driven steel plates, and by comparing the obtained data with those available in the literature.

The velocimeter was applied to the flying plate test. The aim was to find whether the free surface velocity data were suitable to calculate the detonation (Chapman-Jouguet) pressure according to the flying plate technique [4]. The other question to answer was to find the time resolution of the PDV. A nanosecond time resolution should be achieved.

The velocimeter should have been able to detect the propagation of the shockwave in metal, and register its dispersion into several waves termed elastic and plastic [5]. This can also be

accompanied by the phase transition of the shocked metal. The measurement of the wave velocities could allow one to deduce the spallation strength of the metal.

The acceleration of the metal plate and then steadying its velocity was observed. The acceleration of the metal plate depends on the detonation products pressure, thus it is possible to derive an equation of state for the reacted explosive in the cylinder expansion test [6]. The explosively driven metal plate attains its terminal velocity which is a function of the mass of metal and of explosive. A Gurney constant can be derived which is used in the prediction of the velocity of fragments in a detonated warhead [7]. These effects occur on a microsecond scale.

## 2. Experimental

### 2.1 Explosive charge assembly

Mild steel disks of the diameter 30 mm and thickness 5 mm were accelerated by detonation of PE4 charges of mass of 15 g, 30 g, or 60 g placed next to the metal disk. The PE4 charge was hand-packed into a cardboard tube of the inner diameter 28 – 33 mm. The length of the explosive charge varied between 15 – 60 mm. Figure 1 shows the assembly from the steel disk end, and Figure 2 gives the side-on view of the charge.



*Figure 1 View of a typical explosive charge assembly from the steel disk end. The diameter of the steel disk is 30 mm and the length of the assembly is 35 mm (30 mm charge and 5 mm steel disk) encased in a cardboard tube.*



*Figure 2 Side view of the explosive charge assembly encased into a cardboard tube. A steel disk of the thickness 5 mm is located at the bottom of the assembly, and a plastic detonator holder can be seen above it.*

Table 1 shows the list of the firing events when the free surface velocity histories were recorded. In those firings, the distance between the optical fibre tip and the steel target varied between 1 – 4 mm. At distances 8 mm and above, no velocity history could be recorded because the signal was too weak.

*Table 1 List of firing events showing mass of PE4 charges, their corresponding lengths and diameters, and the distances between the optical probe and surface of steel target for each event.*

| Event Number | PE4 charge mass (g) | PE4 charge length (mm) | PE4 charge diameter (mm) | Distance to target (mm) |
|--------------|---------------------|------------------------|--------------------------|-------------------------|
| 110307_02    | 30                  | 25                     | 33                       | 1                       |
| 110308_01    | 30                  | 30                     | 30                       | 2                       |
| 110308_02    | 15                  | 15                     | 30                       | 2                       |
| 110308_03    | 60                  | 60                     | 30                       | 2                       |
| 110308_04    | 30                  | 35                     | 28                       | 4                       |
| 110309_01    | 30                  | 35                     | 28                       | 1.5                     |

## 2.2 Photon Doppler Velocimeter

### 2.2.1 Heterodyne theory

A concept schematic demonstrating in-principle operation of a Photon Doppler Velocimeter is shown in Figure 3.

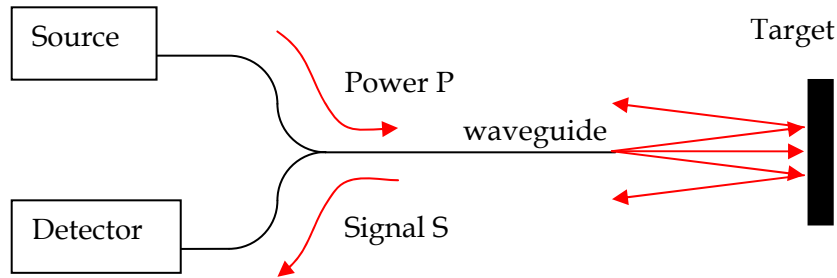


Figure 3 Photon Doppler Velocimeter schematic.

When incident light is reflected from a target surface in close proximity to the end of a fibre optic waveguide some of that reflected light is captured by the waveguide. If the end of the fibre optic waveguide emitting the light is cleaved normal there will be a second Fresnel reflection of around 3.5% from the glass-air interface at the waveguide exit/entrance. If both reflections are coherent they will interfere. It is possible to show that the intensity of the light returning back along the waveguide  $S$  will be given by

$$S = P \left( \left( \frac{(n-1)}{(n+1)} \right)^2 + R + 2\sqrt{R} \frac{(n-1)}{(n+1)} \cos \left( 2\pi \frac{2\mathbf{d} \cdot \hat{\mathbf{n}}}{\lambda} \right) \right) \quad \text{Equation 1}$$

where  $P$  is the power emitted by the fibre,  $R$  is the proportion of the emitted power reflected by the target surface and coupled back into the waveguide,  $n$  is the refractive index of the waveguide,  $\mathbf{d}$  is the distance to the target from the end of the waveguide,  $\hat{\mathbf{n}}$  is a unit vector in the direction the waveguide is aiming and  $\lambda$  is the wavelength of the probe light.

The key feature is that as the distance between the waveguide and the target changes the signal is oscillatory with a cycle corresponding to the change in the target distance  $\mathbf{d}$  by  $\lambda/2$ .

For a moving target it can be seen there will be one oscillation or pulse for every half wavelength of target movement. The frequency of these pulses is thus

$$f = \frac{2}{\lambda} \mathbf{v} \cdot \hat{\mathbf{n}} \quad \text{Equation 2}$$

where  $\mathbf{v}$  is the velocity of the target and  $\hat{\mathbf{n}}$  is a unit vector in the direction the waveguide is aimed.

As an example, if a laser source operating at wavelength  $\lambda = 1.55 \mu\text{m}$  is considered then the signal oscillation frequency from a target with a surface velocity of 1 km/s will be 1.29 GHz. Thus, the maximum velocity measurable is limited by the bandwidth of the data acquisition system.

### 2.2.2 Implementation

A photograph of the Photon Doppler Velocimetry system is shown in Figure 4. It is located outside the explosive chamber. An optical fibre goes from the circulator 3 through the port 6 inside the explosive chamber where it terminates near the steel target and the explosive charge as is shown in Figure 5.

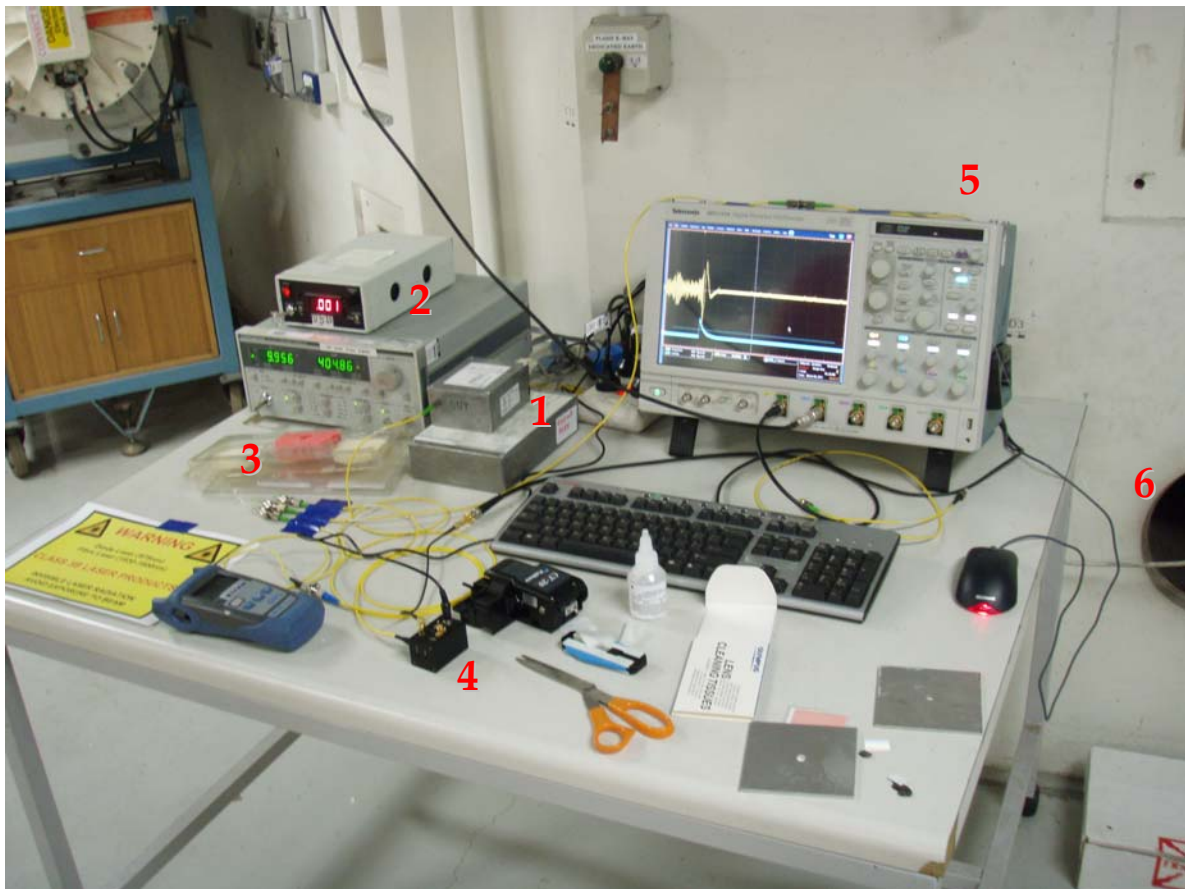


Figure 4 A photograph of the Photon Doppler Velocimeter outside the explosive chamber. 1 – laser and light amplifier, 2 – power supplies for the laser and for the amplifier, 3 – circulator, 4 – photodetector EOT ET-5000AF, 5 – oscilloscope Tektronix DPO7254, 6 – partial view of the port in the explosive chamber wall through which the optical fibre is fed to the target.

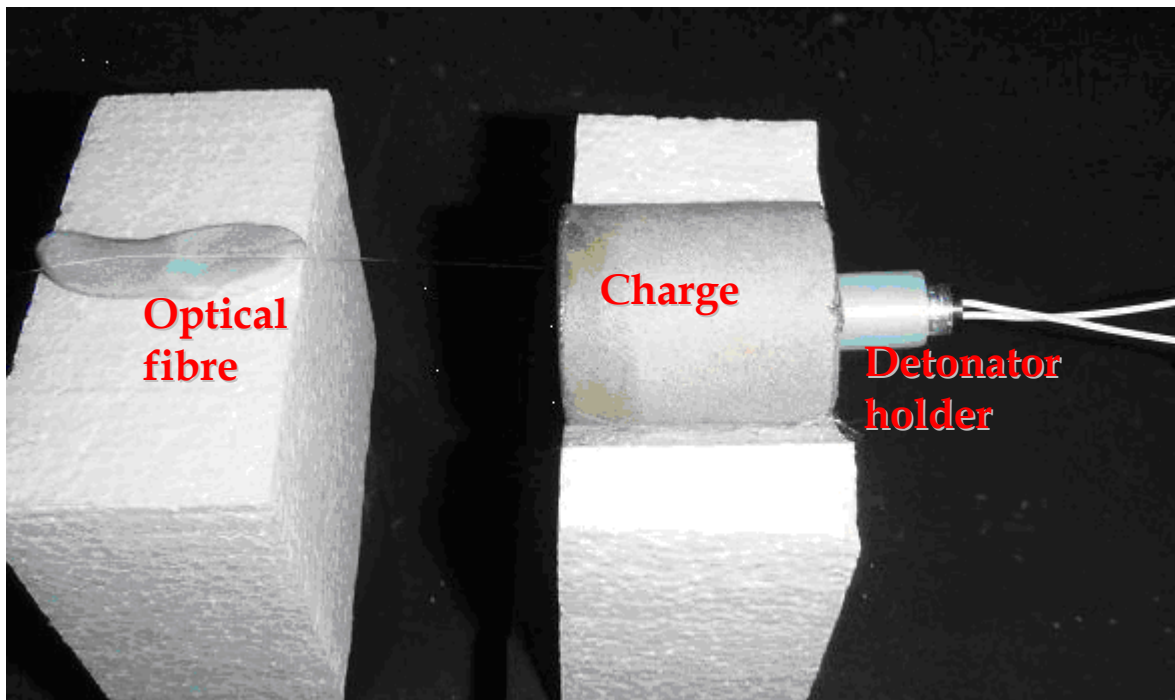


Figure 5 An explosive charge assembly is mounted inside the explosive chamber on right. On left, an optical fibre is mounted with Blu-Tack on a Styrofoam holder, so that the distance between the metal plate surface and the tip of fibre was between 1 – 4 mm.

The optical schematic of the velocimeter is shown in Figure 6.

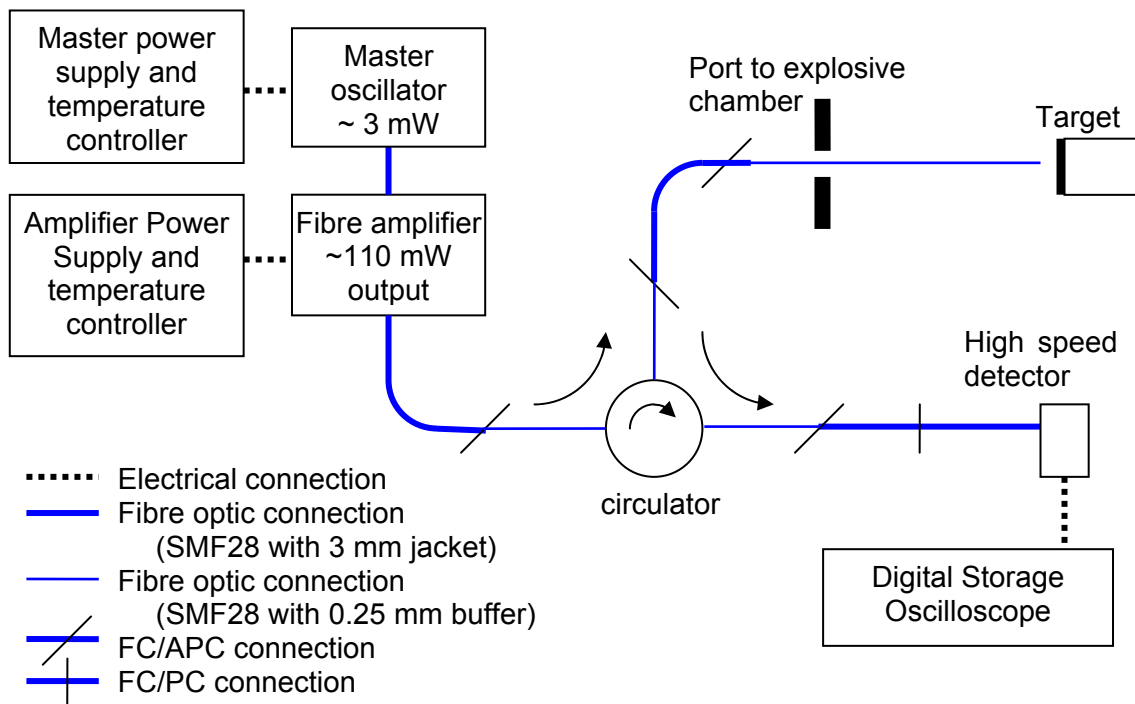


Figure 6 A schematic diagram of Photon Doppler Velocimeter.



The laser source consisted of a master oscillator with a power amplifier which was developed within Electronic Warfare and Radar Division (EWRD) for another project.

The master oscillator module consisted of a single longitudinal mode Erbium (Er) fibre ring laser pigtailed with a length of Er doped fibre to absorb residual pump light in order to further amplify the ring laser output. These were pumped in series by a 350 mW single spatial mode 975 nm pump diode (manufactured by Bookham, Inc). The ring laser module was manufactured by Orbits Lightwave under the product name "Eternal" and with a few mW of pump light produced around 0.5 mW output power with a short term linewidth  $< 3$  kHz. The output from the Er fibre pigtail was passed through a dual stage isolator and terminated with an FC/APC connector resulting in an output of around 3 mW centred at 1550.0 nm. The pump diode was temperature controlled and driven with 400mA by a diode driver from IXL Lightwave.

The power amplifier consisted of a length of around 30 m of Erbium 1550C3 fibre (Corning) counterpumped using a wavelength-division multiplexing (WDM) by a 450 mW single spatial mode 975 nm pump diode (Bookham). This was driven at 600 mA by an internally developed diode driver and temperature controller incorporating the laser diode driver and the temperature controller modules (Wavelength Electronics).

A 3-port optical fibre circulator with central wavelength 1550 nm was purchased from AFW Technologies Pty Ltd. A 2  $\mu$ m Amplified High Speed Detector ET-5000AF with 1.5 GHz bandwidth was supplied by Electro-Optic Technology, Inc. The oscilloscope was Tektronix DPO7254 with 2.5 GHz bandwidth and 20 GS/s sampling rate. The optical connector faces were cleaned with the Cletop Reel Connector Cleaner before assembly.

The following procedure was adopted for preparing the optical probe. The primary coating was removed by the optical fibre cable stripper branded KNIPEX. The remains of the coating were wiped off by a lint-free tissue soaked in isopropyl alcohol. The fibre was cleaved using Fujikura Fiber Optic Cleaver CT-30A. The fibre tip acted as the optical probe.

### 2.2.3 Requirement for coherence

In order to observe interference, light must have a coherence length greater than the path length difference between the beam lines to be interfered. In this case the path length difference is of the order of 10mm and thus a source with a short term linewidth less than 0.24 nm (30 GHz) is required, a very easily met requirement. For longer target-fibre separations narrower linewidth sources are required:

$$\begin{aligned} \text{Coherence length} &> 2d \\ \text{Short term linewidth (e.g. measured over } 100\mu\text{s)} &< \frac{c}{2d} \end{aligned}$$

where  $d$  is the target-fibre separation and  $c$  is the speed of light.

Interfering beams must also have the same state of polarization. Finally, interfering beams must be in the same spatial mode.

#### 2.2.4 Options for increasing the fibre-target range

The preliminary experiments showed that the introduction of an optical probe, e.g. a 15 mm long focal length aspheric lens, could increase the range to the target to approximately 20 mm. This however comes with a cost of increased sensitivity to misalignments both in setup and during detonation.

#### 2.2.5 Laser safety considerations

If the light has a coherence length greater than the path length difference between the two reflections and the polarizations and spatial modes match then the light will behave as if it were a wave. In other words, the product of interference propagates as an electromagnetic wave inside the single-mode fibre.

The tip of the optical fibre is fixed 1 – 4 mm away from the explosively driven metal plate, the velocity of which is to be measured. This tip is the only exit of infrared laser light which is potentially harmful. However, in the explosive environment the fibres are going to potentially get damaged or severed. Ordinarily, the light is emitted with a spread from the fibre, and thus its intensity is below a harmful level for the human eye after propagating a very short distance. The  $1/e^2$  beam diameter from a single mode optical fibre is 10  $\mu\text{m}$  and the full width  $1/e$  divergence is around 100 mrad. This beam has a Nominal Ocular Hazard Distance (NOHD) of 11.3 cm beyond which it is safe for direct viewing without magnifying optics.

It is however possible to collimate the laser using a lens so as to achieve higher signal levels. If one were to use a 15 mm focal length aspheric collimator it is possible to produce a beam with a 3 mm  $1/e^2$  diameter and a 300  $\mu\text{rad}$   $1/e$  diameter divergence. Such a beam would have a 25 m NOHD and would require laser safety glasses with an Optical Density  $\text{OD} \geq 2$  in order to ensure that an operator is safe even in the event of the entire beam being directed into their pupil.

#### 2.2.6 Laser light-explosive interaction

Hazardous interaction of the laser light with the explosive charge is prevented by covering the explosive with inert sheeting material. In the described experiments, the cylindrical PE4 charge was enclosed in the cardboard tube. It was covered by the metal plate on one end, and the plastic detonator holder on the other end, thus no explosive was directly exposed to the laser light.

#### 2.2.7 Data processing

The incident light and the reflected light interfere producing a beat wave. The velocity of the target surface is proportional to the beat frequency and measures in the gigahertz range. It is possible to measure the duration of each cycle, and thus to find the velocity corresponding to the timing of each cycle,

$$\text{velocity (m/s)} = 775/\text{period (ns)}$$

Equation 3

A sub-nanosecond time resolution can theoretically be achieved by inferring the cycle duration from measuring only a part of the cycle.

The other method of analysis uses many consecutive cycles to determine the frequency averaged over those cycles. The frequency is obtained by applying a Fourier transform. This analysis results in a lower time resolution, typically several tens of nanoseconds. A tailored subroutine in MATLAB was written to do the Fast Fourier Transform (FFT).

### 3. Results

#### 3.1 Free surface velocity of metal plate

The experiments were conducted with distances of 1, 2, and 4 mm between the target surface and the optical fibre tip. At a 4 mm distance, the photodetector output signal noticeably deteriorated though the beat frequency was still measurable, and at a distance of 8 mm the useful signal disappeared. Figure 7 shows a fragment of the metal disk which was recovered after the explosive event.



*Figure 7 The optical probe-facing side of a fragment of the metal disk recovered after the explosive event. The fragment's width is about 1 cm.*

It appears that the surface of the target can be less than mirror-like for the operation of the velocimeter.

The photodetector output containing the signal with the beat frequency is shown in Figure 8:

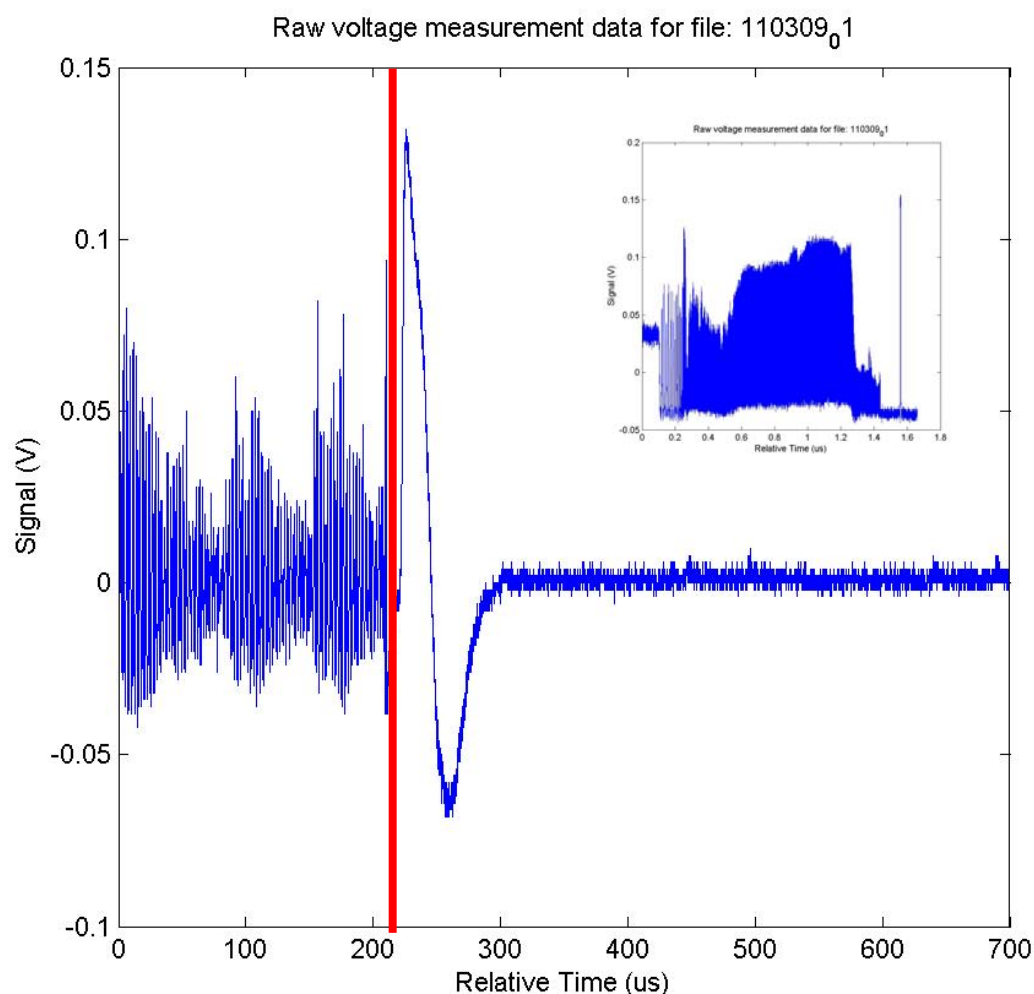


Figure 8 Photodetector output containing the signal with the beat frequency. Only a small fraction of the recorded signal (less than  $2\ \mu\text{s}$ ) contains the useful signal indicated by the vertical red strip and is shown in inset.

An FFT was made on the raw signal and the period with the beat frequency of interest was easily identified. Then the signal was converted back into the time domain. Figure 9 shows the velocity time history of the steel disk accelerated by a 30 g PE4 charge.

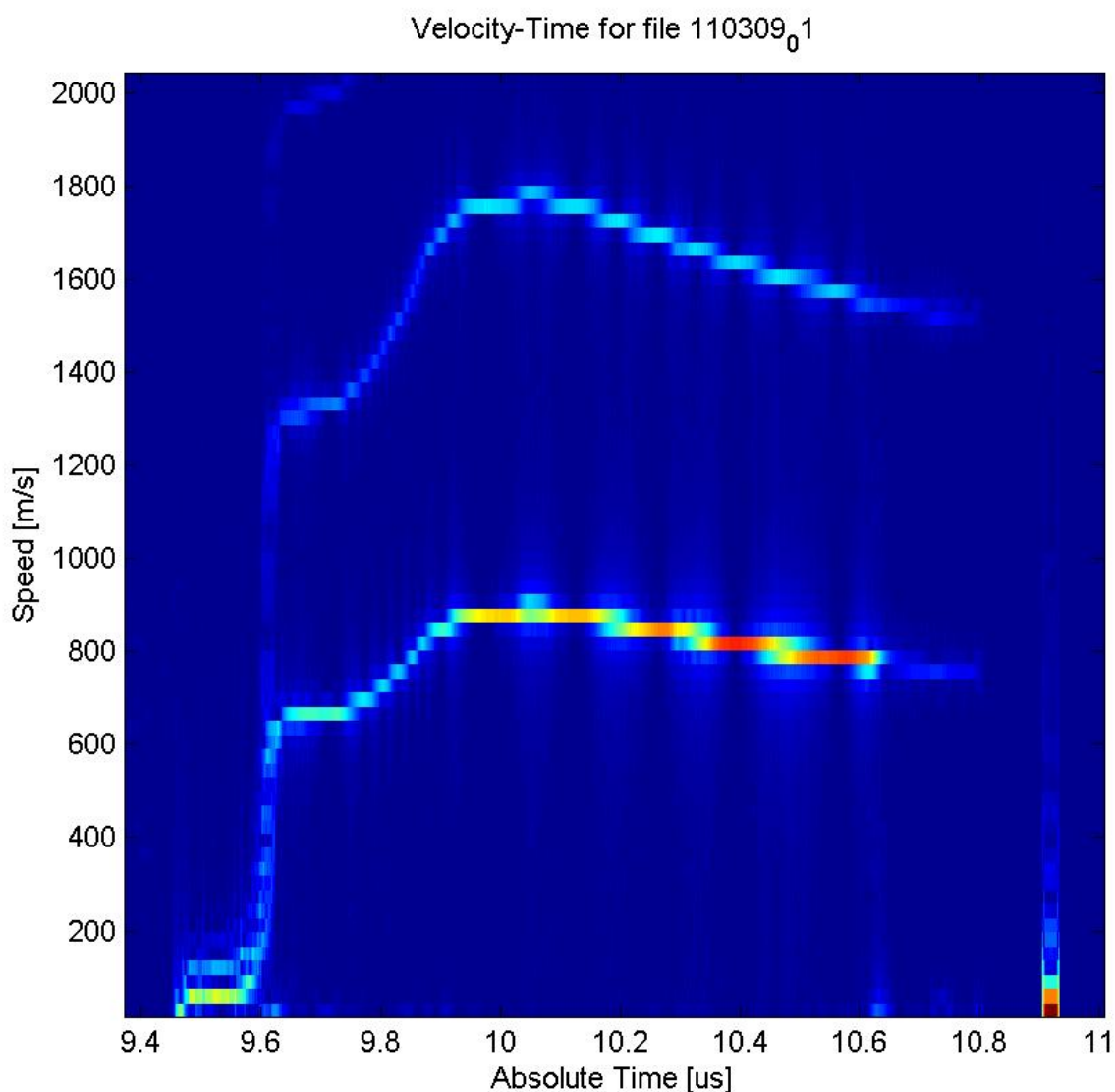


Figure 9 Velocity of a 28 g steel disk accelerated by a 30 g PE4 charge derived by the fast Fourier Transformation method. A window of 40 ns was used for the FFT procedure. The bottom line with a maximum velocity of about 800 m/s is the real signal and the two lines above are harmonics artefacts.

It can be seen that the photodetector signal is weakest at the initial high acceleration part of the graph, where the velocity is changing rapidly, and is strongest after the velocity peaked. A time resolution of 40 ns was employed here, and was determined by the FFT window parameters.

However, for some signals it was possible to distinguish the individual oscillations in the beat frequency. Thus, the target velocity for the duration of the period was found according to Equation 3. Figure 10 shows the velocity of a 28 g steel disk accelerated by 30 g of PE4. The time resolution achieved in this set of experiments was 7 ns.

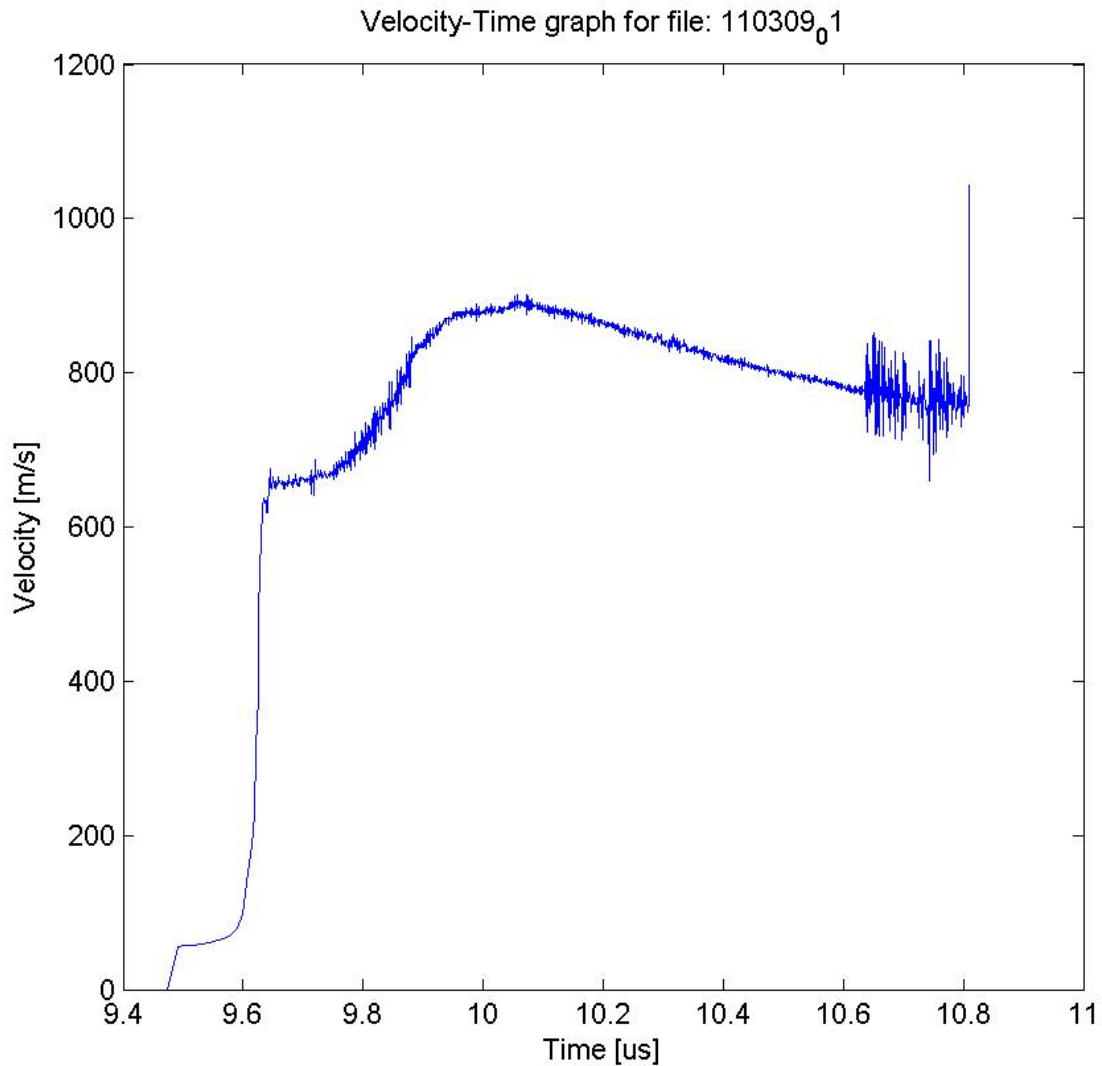


Figure 10 Velocity of the 28 g steel disk determined by calculating the period for each oscillation of beat frequency (same raw data as used in the FFT method of Figure 9). An improved resolution of 7 ns was achieved.

Figure 11 shows the velocity histories determined for six events with the steel disk of a calculated mass of 28 g and with the explosive charge of a mass of 15 g, 30 g, or 60 g. The peak free surface velocities and the steady (final) free surface velocities for those events are shown in Table 2. It is deemed that three of those lines have plateaued, however the recording time was too short for the other three lines (less than 2  $\mu$ s) to definitely claim that they have plateaued.

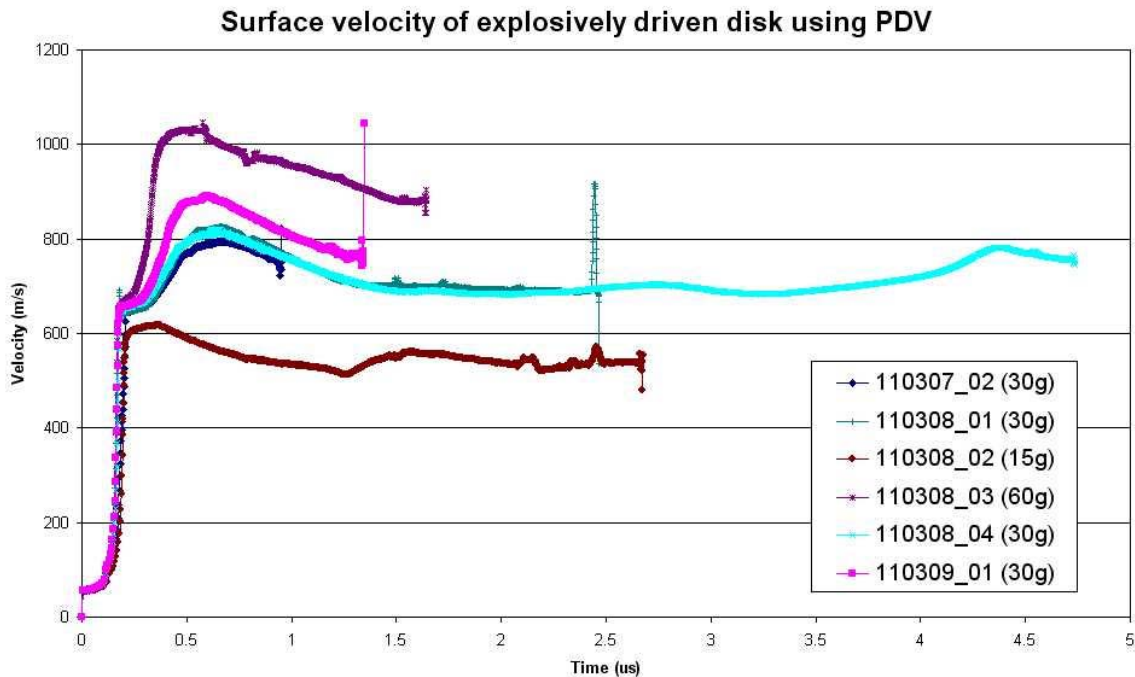


Figure 11 The velocity of a 30 g steel disk accelerated by a PE4 charge of a mass of 15 g, 30 g or 60 g. The diameters of the PE4 charges vary between 28 and 33 mm, and are detailed in Table 1.

Table 2 Results of the six events where a steel disk of a thickness of 5 mm was thrown by a PE4 charge of mass of 15, 30 or 60 g. The free surface velocity attained a peak value ("peak velocity") and then plateaued at a lower value ("final velocity").

| Event No. | PE4 charge mass (g) | Charge length (mm) | Peak velocity (m/s) | Final velocity (m/s) |
|-----------|---------------------|--------------------|---------------------|----------------------|
| 110307_02 | 30                  | 25                 | 800                 | Not achieved         |
| 110308_01 | 30                  | 30                 | 820                 | 700                  |
| 110308_02 | 15                  | 15                 | 620                 | 540                  |
| 110308_03 | 60                  | 60                 | 1030                | 880 (apparently)     |
| 110308_04 | 30                  | 35                 | 820                 | 680                  |
| 110309_01 | 30                  | 35                 | 890                 | 760 (apparently)     |

## 4. Discussion

### 4.1 Elastic and plastic waves in steel

#### 4.1.1 Elastic-plastic model

In the experiment described above, the detonation wave of PE4 propagated through the steel plate and emerged at the free surface. The velocity of the latter was measured. There are

several phenomena associated with the shock compression of steel which are shown in a general sense in Figure 12.

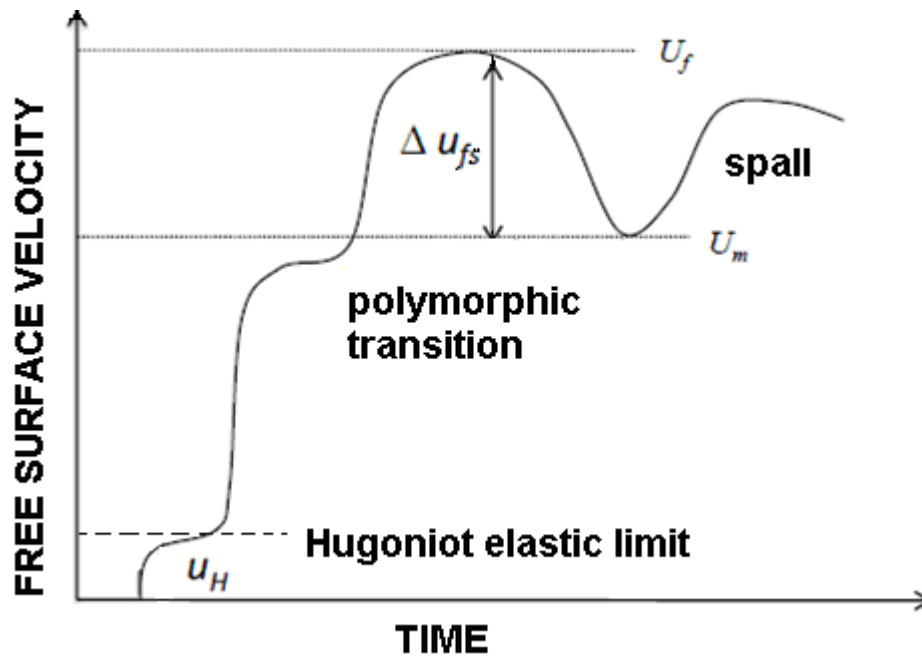


Figure 12 Free surface velocity profile showing the features accompanying the shock compression of steel.

When the detonation wave hits an iron plate, it responds to the shockwave in such a way that the single shockwave breaks up into three waves as was first reported in [5]. (The shock compression features are similar between iron and steel, which consists mostly of iron, as is detailed e.g. in [8].) The first wave is an elastic wave, the second wave is a plastic wave, and the third wave is a phase transforming wave for impact stresses greater than 13 GPa. The authors of Reference 5 first demonstrated it by employing VISAR for the measurement of the time-resolved free surface velocity of shocked iron in [1], and later provided a more detailed investigation [9].

In a steel bar, the elastic wave moves faster than the other waves. It causes an increase in free surface velocity. In these elastic disturbances, the displacement is wholly in the direction of propagation of the waves, and the velocity  $V$  is given by [10]:

$$V = \sqrt{\frac{3K}{\rho} \times \frac{1-\nu}{1+\nu}}$$

Equation 4

where  $K$  is the bulk modulus of compression,  $\rho$  is the density, and  $\nu$  is the Poisson's ratio. For iron, the authors used the values  $1/K = 0.61 \times 10^{-12}$  dynes/cm<sup>2</sup>,  $\rho = 7.8$  g/cm<sup>3</sup>, and  $\nu = 0.28$ . They obtained the velocity of the elastic wave  $V = 5950$  m/s.



Within an elastic-plastic model, a threshold stress called the Hugoniot elastic limit (HEL) is proposed to describe the yielding behaviour of materials, and can be calculated from the formula :

$$\sigma_{HEL} = \rho V u_H / 2 \quad \text{Equation 5}$$

Here,  $\rho$  is the density of steel,  $V$  is the longitudinal sound speed, and  $u_H$  is free surface velocity at  $\sigma_{HEL}$ .

The second major velocity increase results from arrival of the first plastic wave. It has been shown that iron experiences a polymorphic phase transition  $\alpha \leftrightarrow \epsilon$  when subjected to a pressure of about 13 GPa. The first plastic wave corresponds to the onset of the phase transition.

The third major increase in velocity is caused by the phase transition, i.e. the transition of material which carries the material from the  $\alpha$  phase to the  $\epsilon$  phase. In Figure 12, a rise in the velocity to a maximum value  $U_f$  can be seen.

Finally, one may see a relatively small additional free surface velocity increase, called phase interface reflection (PIR). It is caused by the reflection of a release wave from the internal interface between the  $\epsilon$  phase and  $\alpha$  phase. The detailed explanation is available from Barker *et al* [9], Chapter 4D. Additional experiments are required to establish whether the PIR feature exists in these tests.

The compression wave reflects from the free surface of the steel plate as a rarefaction wave. This rarefaction wave pulls back the particles of the metal plate which manifests itself in the reduction of the free surface velocity by  $\Delta u_{fs}$  in Figure 12. The rarefaction wave interacts with the still oncoming rarefaction wave behind the shock, and a high tension in the metal ensues. If the tension is high enough this results in forming a crack inside the metal termed "spall". There could be an oscillation in the free surface velocity which is the "ringing" of the wave trapped inside the spalled piece [1]. The pressure pulse is probably too long for spall to occur.

After the "ringing" subsides, the surface of the metal is moving with the same velocity as the metal plate on the whole. For the description of the plate movement, a simple yet precise theory was developed by Gurney [7]. It will be described in the following section.

#### 4.1.2 Interpretation of free surface velocities

It follows from Figure 11 that the elastic wave in the 5 mm thick steel plate had a velocity of approximately 50 m/s. Applying the Equation 5 for the Hugoniot elastic limit, the HEL stress attained in the experiment was 1.16 GPa. This value fits well by interpolation into the data quoted by Barker *et al* [9] who found that with an elastic wave speed of 6000 m/s, the elastic wave stress was 1.10 GPa for the 6.35 mm thick iron specimens, and 0.92 GPa for the 16 and 19 mm thick specimens. Barker *et al* did not have an overshoot in velocity for the 3.11 mm thick specimen, but they derived it to be 1.3 GPa. It is evident that the velocity step 50 m/s at a time between 0 and 0.2  $\mu$ s obtained with the Photon Doppler Velocimeter corresponds well to the expected value.

At a time of 0.6  $\mu\text{s}$ , there is an inflection point in the free surface velocity. It is common for all of the experiments and is equal to  $660 \text{ m/s} \pm 30 \text{ m/s}$  (except for the experiment with 15 g of PE4 which is discussed separately). The corresponding pressure is calculated below.

Barker *et al* [9] found the Hugoniot for the  $\alpha$  phase which was close to the Hugoniot of steel published elsewhere [11]:

$$u_s = 4.63 + 1.33 u_p \quad \text{Equation 6}$$

Here,  $u_s$  is the shockwave velocity in steel, and  $u_p$  is the particle (mass) velocity in steel. Particle velocity is approximated to be equal to half of the free surface velocity. The application of Equation 5 results in the shock wave velocity of the experiment to be equal to 5070 m/s. The substitution of this value in the impulse conservation equation  $P = \rho u_s u_p$  yields the value 13.1 GPa, which is close to the  $\alpha \leftrightarrow \epsilon$  polymorphic phase transition pressure of 13 GPa. Thus, it is believed that the Photon Doppler Velocimeter was able to resolve correctly the steel free surface velocity corresponding to the iron phase transition.

After the inflection point on the velocity history graph corresponding to the phase transition, the free surface velocity increases until it reaches a maximum value. The peak of the free surface velocity is achieved at the time 0.5 – 0.7  $\mu\text{s}$  being in the range 800 – 1030 m/s (except for the charge with 15 g of PE4 which will be considered separately).

The theory for the attenuation of the shock pulse progressing through material stipulates that the shockwave consists of the region where the pressure suddenly rises, and a release, or rarefaction behind the peak pressure where the pressure returns to zero as is described by Meyers [12], p.183. The rarefaction behind the shock wave travels faster than the shock wave, and when it reaches it, the peak pressure decreases. Obviously, the duration of the rarefaction wave depends on the rarefaction wave formed in the explosive during the expansion of the detonation products (called the Taylor release wave). It appears that the length of the explosive charge (15 – 60 mm) was not enough for the steady detonation wave to establish.

In Figure 13, the peak velocities attained by the steel disk surface are plotted against the lengths of the corresponding PE4 charges. The data are fitted with a quadratic curve. One can see that the peak surface velocity increases at a slowing rate with the length of the charge. It appears when a sufficiently long charge is used, the peak surface velocity would attain its maximum.

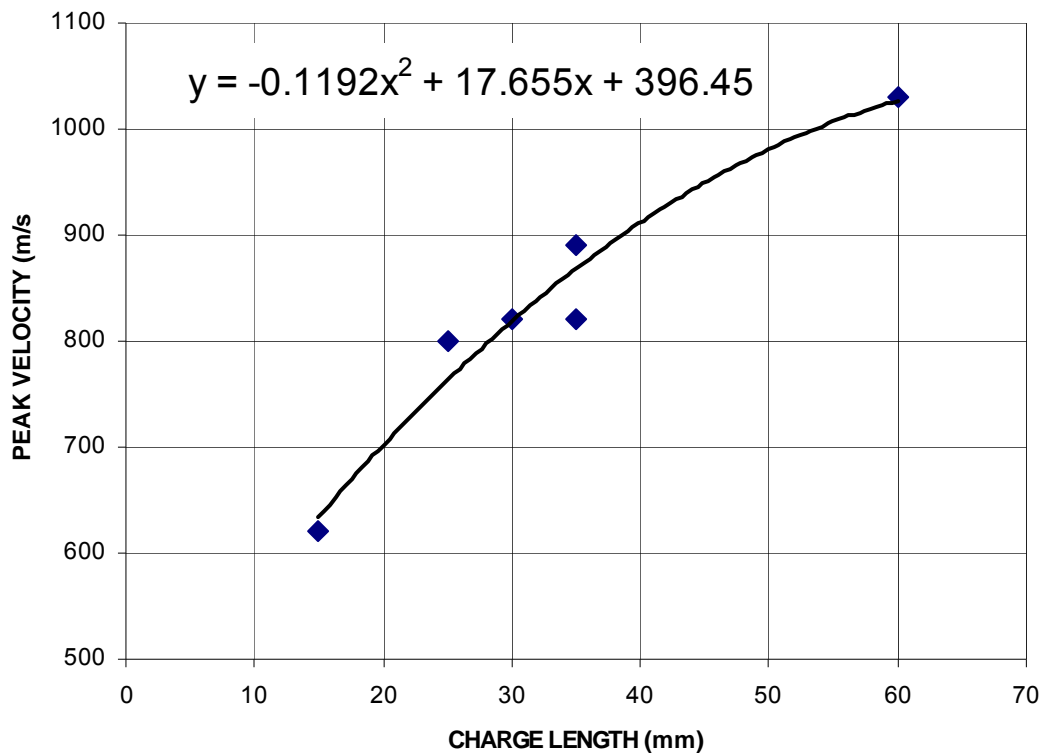


Figure 13 The peak free surface velocities measured in 5 mm thick steel disks driven by the PE4 charges of lengths of 15, 25, 30, 35 and 60 mm. A quadratic curve is fitted to the data.

The C-J pressure of explosive in the flying plate test can be calculated using the Goranson equation [4],

$$P = \frac{1}{2} W_m (\rho_0 D + \rho_{0m} U_m)$$

Equation 7

where  $W_m$  is the metal particle velocity,  $\rho_0$  is the initial density of explosive,  $D$  is the velocity of detonation of explosive,  $\rho_{0m}$  is the initial density of metal, and  $U_m$  is shockwave velocity in metal.

Substituting a maximum measured free surface velocity of 1030 m/s ( $W_m = 515$  m/s) into **Equation 7**, the pressure turns out to be 14.1 GPa. This is significantly less than the C-J pressure of PE4, 21 -- 24 GPa. Obviously, the C-J pressure was not attained in the experiment with a charge of a length of 60 mm.

There is experimental evidence in the scientific literature that the amplitude of the free surface velocity becomes larger with the longer length of the shockwave-driving explosive charges. For example, Hiroe *et al* [13] used 10 mm or 20 mm long PETN charges to drive a shockwave into an adjacent aluminium alloy specimen of length 20 mm. They reported an increased free surface velocity of the metal plates for the longer PETN charges. The authors interpreted this finding by stipulating that the initial loading profile in aluminium alloy plate was triangular

in shape and the rate of pressure decay from the shockwave front was a function of the charge length.

In another example, Seitz *et al* [14] drove shockwaves of varying pressures into a slab of PBX9502 (TATB-based) explosive and measured the free surface velocity history with VISAR. This material has a short detonation reaction zone length, less than 1 – 2 mm. They observed that a steady state of detonation wave in their 50 mm long charges was not achieved. Thus, they theorised, the Chapman-Jouguet state was not observed. It was suggested to use the charges at least 100 mm long.

However, Beaucy *et al* [15] recently reported the results of an experiment similar to that of Seitz. They used both VISAR and PDV to measure the particle velocity history at the interface between a TATB-based PBX charge T2 (45 – 135 mm long) and a LiF or PMMA window (5 mm long). The authors concluded that there was no dependency of the explosive particle velocity on the explosive charge length.

For the 15 g (15 mm long) PE4 charge in Figure 11, the inflection point was reached separately at a velocity of 600 m/s, and then the velocity profile peaked at a velocity of 620 m/s. This free surface velocity corresponds to a plastic wave with velocity 4730 m/s and a pressure of 11.1 GPa. It could be suggested that the length of the charge (15 mm) was not sufficient to establish a long enough loading profile in the steel target. The weaker wave deteriorated quickly in the length of steel (5 mm), and thus reached the free surface at a lower velocity. Barker *et al* [9] attribute a similar result to the low impact velocity of the iron-nosed projectile on their iron targets (case 13 and 14) which failed to produce an “appreciable phase transition”.

In the event 110309\_01 (30 g) in Figure 11, there is a very small increase in free surface velocity at a time of approximately 0.7  $\mu$ s. This might be interpreted as the PIR wave.

## 4.2 Velocity of steel plate

### 4.2.1 Gurney equation

When a cased explosive charge detonates, the casing accelerates outwards under the influence of the shockwave and of the expanding detonation products. Gurney developed a simple method describing how the energy was distributed between the kinetic energy of the expanding gases and the kinetic energy of the expanding metal case [7].

For an opens sandwich configuration, the velocity of the metal plate is described by the equation:

$$\frac{V}{\sqrt{2E}} = \left[ \frac{1 + \left(1 + 2\frac{M}{C}\right)^3}{6\left(1 + \frac{M}{C}\right)} + \frac{M}{C} \right]^{-1/2}$$

Equation 8

where  $V$  is the velocity of the metal plate,  $\sqrt{2E}$  is the Gurney constant for a given explosive,  $M$  is the mass of the metal plate, and  $C$  is the mass of explosive.

#### 4.2.2 Interpretation of plate velocity by Gurney formula

The final velocities of the metal plates depending on the mass of the driving explosive charge are shown in Figure 14. The figure also shows the values for the metal velocities predicted by the Gurney equation.

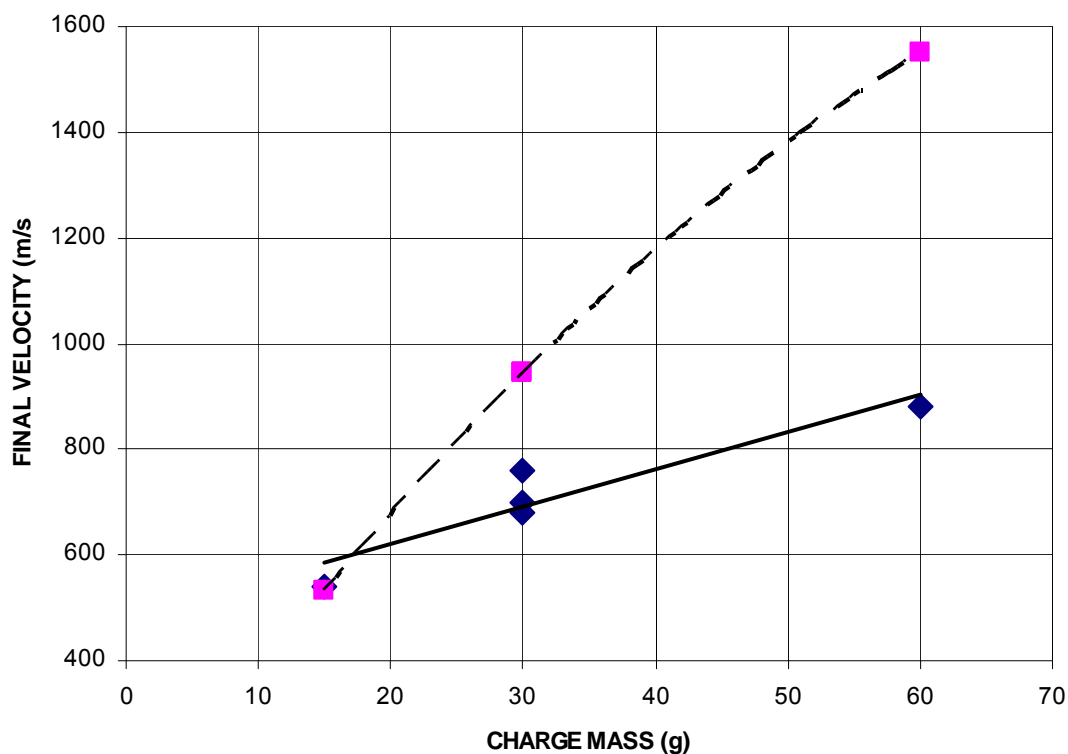


Figure 14 The final steady velocities of the rear surfaces of the 5 mm steel plates explosively driven by 15, 30, and 60 g PE4 charges are denoted by (◆). A straight solid line is fitted. The velocities of the explosively driven steel plates are calculated from the Gurney equation, and is shown as (■). A smoothed dashed line is fitted. The symbols for the measured velocity and the predicted velocity for the 15 g charge overlap.

For the 15 g charge having a length-to-diameter ratio of 1:2, the measured velocity of the metal plate and the predicted velocity are close (540 and 532 m/s correspondingly). However, as the explosive charge becomes longer, the discrepancy between the measured and predicted velocity values becomes more pronounced. For the 60 g charge having the length-to-diameter ratio of 2:1, the measured velocity is somewhat a half of the predicted velocity (880 and 1550 m/s correspondingly). Obviously, in the longer charge, some of the detonation products escape laterally to the sides without contributing to the acceleration of the metal plate.

For the three charges of a mass of 30 g, the measured velocities of the metal plates were in the range 680-760 m/s. Such a discrepancy is probably explained by the fact that the explosive was hand-packed into the cardboard tubes, and thus there might be cavities and density un-uniformities formed between the metal plate and the explosive, which led to the differing gas dynamics.

## 5. Recommendations

### 5.1 Explosives research with Photon Doppler Velocimeter

With the longer explosive charges, one should be able to measure the established C-J pressure in the flying plate test. In a high explosive such as Composition B or PETN, the length of the chemical reaction zone (also known as the von Neumann spike) is well under 1 mm. Thus, if the detonation wave propagates into a metal plate of several millimeters thick, the von Neumann spike is dispersed. The follow-up Taylor wave is attenuated at a much slower rate, so that the pressure at the back side of the flying plate is only few percent less than the pressure at the front side [4]. One could use PDV to measure the free surface velocity of the flying plate back side, and deduce the metal particle velocity at the front side with a high degree of precision. The Goranson equation [4] is used to derive the pressure of the detonation wave in the explosive (Chapman-Jouguet pressure).

As has been shown in the cited literature, PDV could have a nanosecond resolution which would allow resolution of the von Neumann spike and other features in the detonation wave profile. The flying plates should have the thickness much less than the length of the von Neumann spike, i.e. an order of micrometer. Typically, this is realised by the measurement of the velocity of the interface between the explosive and a window. An aluminium layer of a thickness of 1  $\mu\text{m}$  or less is deposited on the surface of the window. Using heavy-density window materials has an added effect that their particle velocity will be slower. In the experiments by Bouyer *et al* [15], the interface explosive/LiF window moves with a maximum velocity of 2200 m/s which is at a maximum capability of the current system. However, a maximum working distance of 4 mm will limit the length of the observable features of the detonation wave to that value. An upgrade of the current laser of the power 100 mW to 2 W could in theory result in the working distance increase to 18 mm.

A possibility to upgrade the capability of PDV is to introduce a lens as the optical probe. However, it was found that the PDV signal deteriorated to unusable with a tilt of the moving surface of around  $10^\circ$ . It was deemed that the laser power should be increased as well in order to make the lens arrangement workable.

In the cylinder expansion test, a copper tube expands under the influence of the detonation products, and the trajectory of the copper walls is recorded. The acceleration of the metal wall is proportional to the pressure of the gaseous detonation products behind the wall. Thus, it is possible to derive the equation of state for the detonation products. The metal wall achieves the terminal velocity after expansion by 1.5 – 2 diameters [16]. Thus, for the equation of state

measurement to occur in an 1-inch diameter copper tube, the working distance should be 12 – 25 mm. This is achievable with the bare fibre as the optical probe and the laser power increased to 2 W.

Since the time of conducting the presented experiments, the authors successfully replaced the in-house laser with the commercially available Koheras AdjustiK C15 (NKT Photonics) of a power output of 100 mW. An option exists to purchase an amplifier module Koheras BoostiK of the power output up to 15 W.

## **6. Conclusions**

A relatively inexpensive and simple Photon Doppler Velocimeter has been developed and has been used to measure the free surface velocities in steel plates. The results are consistent with the previous observations in the literature of shock compression of iron, and with the Gurney model. The velocimeter exhibited robustness of operation provided the distance between the surface of the metal plate and the fibre tip was 4 mm or less.

## **7. Acknowledgements**

The authors are grateful to John Williams who prepared the hand-packed explosive charges and conducted the firings.

## 8. References

1. L.M. Barker and R.E. Hollenbach, "Laser interferometer for measuring high velocities of any reflecting surface", *J. Appl. Phys.* **43**, 4669 (1972).
2. C. F. McMillan, D. R. Goosman, N. L. Parker, L. L. Steinmetz, H. H. Chau, T. Huen, R. K. Whipkey, and S. J. Perry, "Velocimetry of fast surfaces using Fabry-Perot interferometry", *Rev. Sci. Instrum.* **59**, 1 (1988).
3. O.T. Strand, D.R. Goosman, C. Martinez, and T.L. Whitworth, "Compact System for High-Speed Velocimetry Using Heterodyne Techniques", *Rev Sci. Instrum.* **77**, 083108 (2006).
4. W.E. Deal, "Measurement of Chapman-Jouguet Pressure for Explosives", *J. Chem. Phys.* **27**, 796 (1957).
5. D. Bancroft, E. L. Peterson, and S. Minshall, "Polymorphism of Iron at High Pressure", *J. Appl. Phys.* **27**, 291 (1956);
6. J.W. Kury, H.C. Hornig, E.L. Lee, J.L. McDonnell, D.L. Ornellas, M. Finger, F.M. Strange, and M.L. Wilkins, "Metal Acceleration by Chemical Explosives", *Proc. 4th. Int. Symp. on Detonation*, 3-13, (1965).
7. R.W. Gurney, "The initial Velocities of Fragments from Bombs, Shells, and Grenades", Army Ballistic Research Laboratory Report BRL 405, 1943.
8. N.Bourne and J.Millett, "Contrasting the Shock Properties of Iron and Steel", *Scripta Mater.* **43**, 541 (2000).
9. L.M. Barker and R. E. Hollenbach, "Shock wave study of the  $\alpha \leftrightarrow \epsilon$  phase transition in iron", *J. Appl. Phys.* **45**(11) 4872 (1974).
10. D. C. Pack, W. M. Evans and H. J. James, "The Propagation of Shock Waves in Steel and Lead", *Proc. Phys. Soc.* **60** 1 (1948).
11. Stanley P. Marsh, "LASL Shock Hugoniot Data", University of California Press, 1980.
12. Marc M. Meyers, "Dynamic Behavior of Materials", John Wiley & Sons, 1994.
13. T. Hiroe, K. Fujiwara, H. Matsuo, Y. Aaraki and D. Nakayama, "Dynamic Responses of Plates and Cylinders Impacted with Detonation Gases Initiated Using Wire Explosion Techniques", Transactions of the 15<sup>th</sup> International Conference on Structural Mechanics in Reactor Technology (SMiRT-15), Seoul, Korea, 15-20 August 1999.
14. W. L. Seitz, H. L. Stacy, R. Engelke, P. K. Tang, and J. Wackerle, "Detonation Reaction-Zone Structure of PBX9502", Ninth Symposium (International) on Detonation, Portland, Oregon, 28 August - 1 September 1989.



15. V. Bouyer, M. Doucet and L. Decaris, "Experimental measurements of the detonation wave profile in a TATB based explosive", International Workshop: New Models and Hydrocodes for Shock Wave Processes in Condensed Matter, Paris, France, 24-28 May 2010.
16. C. Rumchik, R. Nep, G.C. Butler, B. Breaux, and C. Lindsay, "The miniaturization and reproducibility of the cylinder expansion test", *AIP Conf. Proc.* **1426**, 450 (2012).

|  |                          |                             |  |   |  |                                  |  |
|--|--------------------------|-----------------------------|--|---|--|----------------------------------|--|
| DEFENCE SCIENCE AND TECHNOLOGY ORGANISATION<br>DOCUMENT CONTROL DATA   |                          |                             |  | 1. PRIVACY MARKING/CAVEAT (OF DOCUMENT)   |  |                                  |  |
|  |                          |                             |  |   |  |                                  |  |
| 2. TITLE<br><br>Development of Photon Doppler Velocimeter for Explosives Research  |                          |                             |  | 3. SECURITY CLASSIFICATION (FOR UNCLASSIFIED REPORTS THAT ARE LIMITED RELEASE USE (L) NEXT TO DOCUMENT CLASSIFICATION)<br><br>Document (U)<br>Title (U)<br>Abstract (U) |  |                                  |  |
| 4. AUTHOR(S)<br><br>Valerian A. Kuznetsov and Shayne P. Bennetts   |                          |                             |  | 5. CORPORATE AUTHOR<br><br>DSTO Defence Science and Technology Organisation<br>PO Box 1500<br>Edinburgh South Australia 5111 Australia                                  |  |                                  |  |
| 6a. DSTO NUMBER<br>DSTO-TR-2792  |                          | 6b. AR NUMBER<br>AR-015-494 |  | 6c. TYPE OF REPORT<br>Technical Report  |  | 7. DOCUMENT DATE<br>January 2013 |  |
| 8. FILE NUMBER<br>-  | 9. TASK NUMBER<br>07/372 | 10. TASK SPONSOR<br>CWSD    |  | 11. NO. OF PAGES<br>22  |  | 12. NO. OF REFERENCES<br>16      |  |
| DSTO Publications Repository<br><br><a href="http://dspace.dsto.defence.gov.au/dspace/">http://dspace.dsto.defence.gov.au/dspace/</a>  |                          |                             |  | 14. RELEASE AUTHORITY<br><br>Chief, Weapons Systems Division  |  |                                  |  |
| 15. SECONDARY RELEASE STATEMENT OF THIS DOCUMENT<br><br><i>Approved for public release</i>   |                          |                             |  |   |  |                                  |  |
| OVERSEAS ENQUIRIES OUTSIDE STATED LIMITATIONS SHOULD BE REFERRED THROUGH DOCUMENT EXCHANGE, PO BOX 1500, EDINBURGH, SA 5111  |                          |                             |  |   |  |                                  |  |
| 16. DELIBERATE ANNOUNCEMENT<br><br>No Limitations  |                          |                             |  |   |  |                                  |  |
| 17. CITATION IN OTHER DOCUMENTS Yes  |                          |                             |  |   |  |                                  |  |
| 18. DSTO RESEARCH LIBRARY THESAURUS<br><br>Photon Doppler Velocimeter, detonation, explosive, PE4  |                          |                             |  |   |  |                                  |  |
| 19. ABSTRACT<br>A Photon Doppler Velocimeter (PDV) was built for explosives research. The PDV is comprised of a 1550 nm continuous-wave single-mode fibre laser, an optical circulator, a photodetector and a GHz range capable oscilloscope. As a test, it was used to record the velocity history of the back surface of 5 mm thick steel plates driven by the detonation products of PE4 charges of mass 15 - 60 g. A bare fibre tip, located 1 - 4 mm away from the target was used as the optical probe. Time resolution of 7 ns was achieved. The free surface velocity effects were interpreted in terms of the elastic-plastic model of steel, Chapman-Jouguet pressure was evaluated, and Gurney equations were applied to describe the motion of the steel plate. The measurement limitations of the PDV system are determined, applications for explosives research are discussed, and the upgrade pathway is recommendedd. |                          |                             |  |   |  |                                  |  |